JAMI
Journal of Applied Mathematics and Informatics

J. Appl. Math. & Informatics Vol. **42***(2024), No. 4, pp. 945 - 968*
https://doi.org/10.14317/jami.2024.945

IMPLEMENTATION OF LAPLACE ADOMIAN DECOMPOSITION AND DIFFERENTIAL TRANSFORM METHODS FOR SARS-COV-2 MODEL

N. JEEVA, K.M. DHARMALINGAM, S.E. FADUGBA*,
M.C. KEKANA, A.A. ADENIJI

Abstract. This study focuses on SIR model for SARS-CoV-2. The SIR model classifies a population into three compartments: susceptible $S(t)$, infected $I(t)$, and recovered $R(t)$ individuals. The SARS-CoV-2 model considers various factors, such as immigration, birth rate, death rate, contact rate, recovery rate, and interactions between infected and healthy individuals to explore their impact on population dynamics during the pandemic. To analyze this model, we employed two powerful semi-analytical methods: the Laplace Adomian decomposition method (LADM) and the differential transform method (DTM). Both techniques demonstrated their efficacy by providing highly accurate approximate solutions with minimal iterations. Furthermore, to gain a comprehensive understanding of the system behavior, we conducted a comparison with the numerical simulations. This comparative analysis enabled us to validate the results and to gain valuable understanding of the responses of SARS-CoV-2 model across different scenarios.

AMS Mathematics Subject Classification : 34E05, 34E10, 65L05.
Key words and phrases : SARS-CoV-2, SIR model, Laplace Adomian decomposition method (LADM), differential transform method (DTM), mathematical modeling, numerical simulation.

1. Introduction

SARS-CoV-2, a novel coronavirus, has caused a worldwide outbreak of the coronavirus disease 2019 (COVID-19). The virus was first identified in Wuhan, China, in December 2019 and has since spread globally, leading to a widespread pandemic [1]. Belonging to the coronavirus family, SARS-CoV-2 is known to

Received January 24, 2024. Revised March 12, 2024. Accepted April 22, 2024. *Corresponding author

cause respiratory illnesses in both animals and humans [2]–[7]. Extensive research is currently dedicated to gaining deeper insights into SARS-CoV-2, focusing on understanding the virus, developing effective treatments, and implementing preventive measures to prevent future outbreaks via mathematical models [8]–[9]. The SIR model, a well-established mathematical epidemiological framework, has been widely utilized to analyze the transmission of infectious diseases within a population. The term "SIR" represents three compartments in which individuals in the population are classified as: Susceptible, Infected, and Recovered. Through a set of differential equations, the SIR model captures the dynamic interplay among these compartments over time, providing valuable insights into disease transmission and progression [12]–[13]. To specifically study the transmission and spread of COVID-19 caused by SARS-CoV-2, the SIR COVID model was developed as a modified version of the classical SIR model. This adapted model has demonstrated its efficacy in analyzing and predicting the spread of COVID-19 in various populations. It plays a crucial role in assessing the impact of interventions, such as social distancing, vaccination campaigns, and quarantine measures, on controlling the spread of the virus. Moreover, the SIR COVID model serves as an indispensable tool for guiding public health strategies and decision-making and enhancing the management and control of the ongoing pandemic. In conclusion, both SARS-CoV-2 and the SIR COVID model are instrumental in comprehending and combating the COVID-19 pandemic. Continuous efforts in research and modeling have contribute to the development of more effective strategies for public health and disease management [14]–[18].

This novel mathematical model for SARS-CoV-2 represents an innovative approach aimed at gaining deeper insights into the transmission dynamics of the virus and its effects on the population during the ongoing COVID-19 pandemic. By considering factors such as immigration, protective measures, exposure rate, cure rate, and interactions between infected and healthy individuals, this model seeks to understand the dynamics andimpact of the pandemic comprehensively [19].

Analytical approaches assist in resolving challenging mathematical problems by combining numerical analysis with analytical accuracy. These strategies are extremely helpful for dealing with nonlinearity and system complexity. Analytical expressions and numerical computations provide precise and effective solutions to real-world challenges across various domains. The Laplace Adomian decomposition method (LADM) is a powerful hybrid technique that merges the Laplace transform and Adomian decomposition method (ADM) for solving differential equations, especially those involving nonlinearity. Its application offers enhanced efficiency and accuracy compared to traditional methods. One significant advantage of LADM is its ability to handle nonlinear differential equations without the need for linearization, perturbation, transformation, or discrimination. This characteristic streamlines the problem-solving process and allows more precise

results. LADM provides an analytical solution represented as a rapidly convergent infinite power series with easily computable terms. This feature contributes to its applicability to a wide range of scientific and engineering domains [20]–[23]. Its success is evident in various fields, such as fluid dynamics, heat transfer, population dynamics, and more, where LADM has been effectively applied to address complex problems and deliver valuable insights [24]–[26]. Its versatility and accuracy make it a valuable tool for researchers and practitioners seeking robust solutions for challenging differential equations in diverse applications.

Differential transform method (DTM) is a semi-analytical approach that utilizes the Taylor series expansion concept. The primary strategy involves transforming the derivatives from the original differential equation into discrete difference equations, which are then addressed through iterative methods. The Numerical approach of DTM for solving nonlinear equations was studied by [27]. Subsequently, this approach has been effectively applied to solve various mathematical problems [29]-[30]. In the study by Harir et al. [28], the authors applied the DTM to solve an SEIR model specific to COVID-19. Through a comparative analysis with the RK4 technique, the efficacy of the DTM was demonstrated. In a study conducted by Adeniji [31], the DTM alongside LADM was employed to address a rotavirus model, and the study provided a thorough explanation of the convergence of DTM in system of nonlinear equations. The Differential transform method offers several advantages, including the simplicity of computation and ease of checking the accuracy of the approximate solution. Using this method, the approximate solution can be easily verified by computing the residuals through straightforward direct substitution.

The primary aim of this study was to employ semi-analytical methods to solve and analyse the SARS-CoV-2 model. Semi-analytical solutions are derived using two powerful methods: the Laplace Adomian decomposition method (LADM) and differential transform method (DTM). These techniques provide highly accurate results with minimal iterations, making them valuable tools for analyzing the dynamics of the SARS-CoV-2 model. The LADM involves breaking down the equations into an infinite power series of Adomian polynomials, facilitating the computation of approximate solutions for the variables of the model. On the other hand, the DTM utilizes Taylor series expansion to approximate the solutions, streamline the analysis process and enhance the computational efficiency. This paper is structured as follows: Section 2 provides the mathematical model for SARS-CoV-2. We solve the system of nonlinear equations through the applications of the Laplace Adomian decomposition and differential transform methods in section 3. We show the model's numerical simulation, tables, graphs and discussions for controlling the disease in sections 4 and 5. Section 6 outlines the conclusions of the paper.

2. Governing system of equation

In this section, we consider the SIR SARS-CoV-2 model proposed by Tong et al. [19], which is expressed in the form (1). This involves dividing the entire population N(t) into three distinct classes: Susceptible $S(t)$, Infected $I(t)$, and Recovered $R(t)$. This division enables us to formulate the ordinary differential equation (ODE) system using the following equations.

$$\begin{aligned} \frac{dS}{dt} &= \wedge + \eta - \chi S - bSI \\ \frac{dI}{dt} &= bSI + \gamma - (\rho + \chi + \xi)I \\ \frac{dR}{dt} &= \xi I - \chi R \end{aligned} \tag{1}$$

with the initial conditions:

$$S(0) = p_1, \quad I(0) = p_2, \quad R(0) = p_3 \tag{2}$$

where $\wedge$ represents the birth rate, η represents the rate of individuals immigrating to the susceptible class, χ represents the natural death rate, b represents the contact rate, γ represents the rate of individuals immigrating to the infected class, ρ denotes the death rate due to coronavirus, ξ denotes the recovery rate. These parameters play crucial roles in understanding the dynamics and behavior of the SARS-CoV-2 model. The dynamics of system (1) are shown in the following flow-chart.

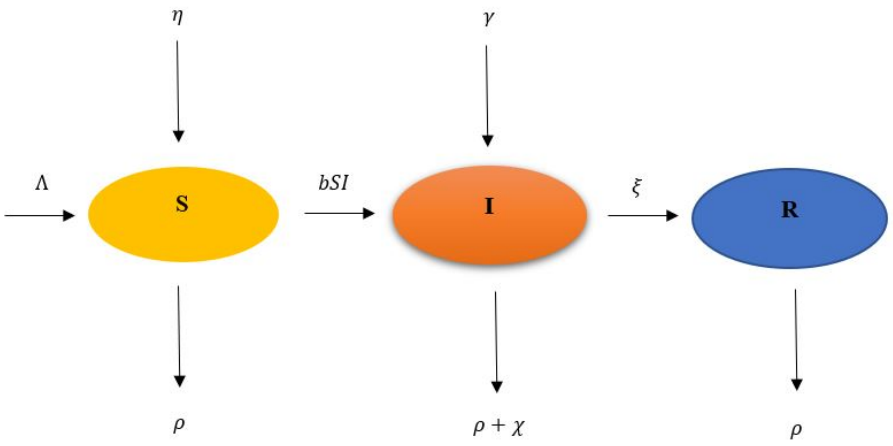

FIGURE 1. Flow chart of SARS-CoV-2 model

TABLE 1. Parameters and their values [19]

Parameter	Value
ρ	0.02
χ	0.0062
$\wedge$	0.6
b	0.0002
γ	0.00097
η	0.00031
ξ	0.003
p_1	222.002105
p_2	0.537176
p_3	0.482

As (1) lacks an exact solution, we provide an semi-analytical solutions by employing the LADM and DTM. For computational purposes, a systematic analysis was conducted using MATLAB and MAPLE.

3. Semi-analytical solutions for the SARS-CoV-2 model

3.1. Laplace Adomian decomposition method (LADM). In this subsection, we demonstrate the application of the Laplace Adomian decomposition method to the nonlinear ordinary differential system (1). To initiate the process, we apply the Laplace transformation, denoted by L, to both sides of the SARS-CoV-2 model.

$$\begin{aligned} L[\frac{dS}{dt}] &= L[\wedge] + L[\eta] - L[\chi S] - L[bSI] \\ L[\frac{dI}{dt}] &= L[bSI] + L[\gamma] - L[(\rho + \chi + \xi)I] \\ L[\frac{dR}{dt}] &= L[\xi I] - L[\chi R] \end{aligned} \tag{3}$$

By using the Laplace transformation properties, we obtain:

$$\begin{aligned} wL[S] - S[0] &= \frac{(\wedge + \eta)}{w} - \chi L[S] - bL[SI] \\ wL[I] - I[0] &= bL[SI] + \frac{\gamma}{w} - (\rho + \chi + \xi)L[I] \\ wL[R] - R[0] &= \xi L[I] - \chi L[R] \end{aligned} \tag{4}$$

Upon applying the initial conditions (2), we obtain:

$$\begin{aligned} L[S] &= \frac{p_1}{w} + \frac{(\wedge + \eta)}{w^2} - \frac{\chi}{w}L[S] - \frac{b}{w}L[SI] \\ L[I] &= \frac{p_2}{w} + \frac{b}{w}L[SI] + \frac{\gamma}{w^2} - \frac{(\rho + \chi + \xi)}{w}L[I] \\ L[R] &= \frac{p_3}{w} + \frac{\xi}{w}L[I] - \frac{\chi}{w}L[R] \end{aligned} \tag{5}$$

Now, we assume that the solutions for S, I and R can be represented in the form of an infinite series, and that the nonlinear terms involving $SI = A$ in the model are decomposed using Adomian polynomials, which are expressed as follows:

$$S = \sum_{n=0}^{\infty} S_n, \quad I = \sum_{n=0}^{\infty} I_n, \quad R = \sum_{n=0}^{\infty} R_n, \quad A = \sum_{n=0}^{\infty} A_n \tag{6}$$

The Adomian polynomials, denoted by A_n, are defined as follows:

$$\begin{aligned} A_n(t) &= \frac{1}{n!}\frac{d^n}{d\lambda^n}[\sum_{i=0}^{\infty}\lambda^i S_i \sum_{i=0}^{\infty}\lambda^i I_i] \\ A_0 &= S_0 I_0 \\ A_1 &= S_0 I_1 + S_1 I_0 \\ A_2 &= S_0 I_2 + S_1 I_1 + S_2 I_0 \end{aligned} \tag{7}$$

Substitute (6) and (7) in (5) to obtain (8):

$$\begin{aligned} L[\sum_{n=0}^{\infty} S_n] &= \frac{p_1}{w} + \frac{(\wedge + \eta)}{w^2} - \frac{\chi}{w}L[\sum_{n=0}^{\infty} S_n] - \frac{b}{w}L[\sum_{n=0}^{\infty} A_n] \\ L[\sum_{n=0}^{\infty} I_n] &= \frac{p_2}{w} + \frac{b}{w}L[\sum_{n=0}^{\infty} A_n] + \frac{\gamma}{w^2} - \frac{(\rho + \chi + \xi)}{w}L[\sum_{n=0}^{\infty} I_n] \\ L[\sum_{n=0}^{\infty} R_n] &= \frac{p_3}{w} + \frac{\xi}{w}L[\sum_{n=0}^{\infty} I_n] - \frac{\chi}{w}L[\sum_{n=0}^{\infty} R_n] \end{aligned} \tag{8}$$

Taking Laplace inverse of (8) to obtain (9):

$$\begin{aligned} \sum_{n=0}^{\infty} S_n &= L^{-1}[\frac{p_1}{w} + \frac{(\wedge + \eta)}{w^2} - \frac{\chi}{w}L[\sum_{n=0}^{\infty} S_n] - \frac{b}{w}L[\sum_{n=0}^{\infty} A_n]] \\ \sum_{n=0}^{\infty} I_n &= L^{-1}[\frac{p_2}{w} + \frac{b}{w}L[\sum_{n=0}^{\infty} A_n] + \frac{\gamma}{w^2} - \frac{(\rho + \chi + \xi)}{w}L[\sum_{n=0}^{\infty} I_n]] \\ \sum_{n=0}^{\infty} R_n &= L^{-1}[\frac{p_3}{w} + \frac{\xi}{w}L[\sum_{n=0}^{\infty} I_n] - \frac{\chi}{w}L[\sum_{n=0}^{\infty} R_n]] \end{aligned} \tag{9}$$

Comparing both sides of the (9), the initial iteration of the Laplace Adomian decomposition is obtained as:

$$\begin{aligned} S_0 &= L^{-1}[\frac{p_1}{w} + \frac{(\wedge+\eta)}{w^2}] \\ I_0 &= L^{-1}[\frac{p_2}{w} + \frac{\gamma}{w^2}] \\ R_0 &= L^{-1}[\frac{p_3}{w}] \end{aligned} \tag{10}$$

(or)

$$\begin{aligned} S_0 &= p_1 + (\wedge+\eta)t \\ I_0 &= p_2 + \gamma t \\ R_0 &= p_3 \end{aligned} \tag{11}$$

The first iteration of the Laplace Adomian decomposition is derived by comparing both sides of the (9):

$$\begin{aligned} S_1 &= L^{-1}[-\frac{\chi}{w}L[S_0] - \frac{b}{w}L[A_0]] \\ I_1 &= L^{-1}[\frac{b}{w}L[A_0] - \frac{(\rho+\chi+\xi)}{w}L[I_0]] \\ R_1 &= L^{-1}[\frac{\xi}{w}L[I_0] - \frac{\chi}{w}L[R_0]] \end{aligned} \tag{12}$$

(or)

$$\begin{aligned} S_1 &= L^{-1}[-\frac{\chi p_1}{w^2} - \frac{(\chi(\wedge+\eta)+bp_1p_2)}{w^3} - \frac{bp_1\gamma + bp_2(\wedge+\eta)}{w^4} - \frac{b\gamma(\wedge+\eta)}{w^5}] \\ I_1 &= L^{-1}[-\frac{(\rho+\chi+\xi)p_2}{w^2} + \frac{bp_1p_2 - (\rho+\chi+\xi)\gamma}{w^3} + \frac{bp_1\gamma + bp_2(\wedge+\eta)}{w^4} \\ &\quad + \frac{b\gamma(\wedge+\eta)}{w^5}] \\ R_1 &= L^{-1}[\frac{\xi p_2 - \chi p_3}{w^2} + \frac{\xi\gamma}{w^3}] \end{aligned} \tag{13}$$

(or)

$$\begin{aligned} S_1 &= -\chi p_1 t - \frac{(\chi(\wedge+\eta)+bp_1p_2)t^2}{2!} - \frac{bp_1\gamma + bp_2(\wedge+\eta)t^3}{3!} \\ &\quad - \frac{b\gamma(\wedge+\eta)t^4}{4!} \\ I_1 &= -(\rho+\chi+\xi)p_2 t + \frac{bp_1p_2 - (\rho+\chi+\xi)\gamma t^2}{2!} + \frac{bp_1\gamma + bp_2(\wedge+\eta)t^3}{3!} \\ &\quad + \frac{b\gamma(\wedge+\eta)t^4}{4!} \\ R_1 &= (\xi p_2 - \chi p_3)t + \frac{\xi\gamma t^2}{2!} \end{aligned} \tag{14}$$

Similarly, the second iteration of the Laplace Adomian decomposition is derived by comparing both sides of the (9):

$$\begin{aligned} S_2 &= L^{-1}[-\frac{\chi}{w}L[S_1] - \frac{b}{w}L[A_1]] \\ I_2 &= L^{-1}[\frac{b}{w}L[A_1] - \frac{(\rho+\chi+\xi)}{w}L[I_1]] \\ R_2 &= L^{-1}[\frac{\xi}{w}L[I_1] - \frac{\chi}{w}L[R_1]] \end{aligned} \tag{15}$$

(or)

$$\begin{aligned} S_2 = L^{-1}[&\frac{\chi^2 p_1}{w^3} + \frac{(-b(\rho+\chi\xi)p_1p_2) + \chi^2(\wedge+\eta)}{w^4} + \frac{(\wedge+\eta)^2b^2\gamma}{w^8} \\ &+\frac{b^2((\eta+\wedge-\gamma)p_2+2p_1\gamma)(\wedge+\eta)}{w^7} + \frac{(-b^2p_1{p_2}^2 - b^2p_2(\wedge+\eta)^2)}{w^5} \\ &+\frac{((-p_1\gamma-(\wedge+\eta)(\rho+\chi+\xi))p_2 - p_1(\rho+\chi+\xi))b - \chi\gamma(\wedge+\eta))}{w^5} \\ &+\frac{b(2p_1p_2(\wedge+\eta)b - ((\rho+\xi)\wedge+{p_1}^2+\eta(\rho+\xi)))\gamma}{w^6}] \end{aligned} \tag{16}$$

$$\begin{aligned} I_2 = L^{-1}[&\frac{(b^2p_1{p_2}^2 + (-p_1(\xi+\rho-p_2)\gamma + \chi(\wedge+\eta)p_2+p_2)b}{w^5} \\ &+\frac{p_1(\rho+\chi+\xi)b}{w^5} + \frac{b^2p_2(\wedge+\eta)^2+\chi\gamma(\wedge+\eta))}{w^5} - \frac{(\wedge+\eta)^2b^2\gamma}{w^8} \\ &+\frac{(\rho+\chi+\xi)^2p_2}{w^3} + \frac{b\chi p_1p_2+(\rho+\chi+\xi)^2\gamma}{w^4} - \frac{b(2p_2(\wedge+\eta)b-p_1\gamma)p_1}{w^6} \\ &-\frac{(-b^2((2p_1-p_2)\gamma+p_2(\wedge+\eta))(\wedge+\eta))}{w^7}] \\ R_2 = L^{-1}[&\frac{bp_2p_1\xi - \xi(\rho+\chi+\xi)\gamma - \chi\gamma\xi}{w^4} + \frac{\xi p_1\gamma b + \xi(\wedge+\eta)p_2b}{w^5} \\ &+\frac{\xi(\wedge+\eta)\gamma b}{w^6} - \frac{(\xi(\rho+\chi+\xi)p_2+\chi\xi p_2-\chi^2p_3}{w^3}] \end{aligned} \tag{17}$$

(or)

$$\begin{aligned} S_2 = &\frac{\chi^2p_1t^2}{2!} + \frac{((-b(\rho+\chi\xi)p_1p_2)+\chi^2(\wedge+\eta))t^3}{3!} + \frac{((\wedge+\eta)^2b^2\gamma)t^7}{7!} \\ &+\frac{(b^2((\eta+\wedge-\gamma)p_2+2p_1\gamma)(\wedge+\eta))t^6}{6!} + \frac{((-b^2p_1{p_2}^2 - b^2p_2(\wedge+\eta)^2)t^4)}{4!} \\ &+\frac{(((-p_1\gamma-(\wedge+\eta)(\rho+\chi+\xi))p_2 - p_1(\rho+\chi+\xi))b - \chi\gamma(\wedge+\eta))t^4)}{4!} \\ &+\frac{(b(2p_1p_2(\wedge+\eta)b - ((\rho+\xi)\wedge+{p_1}^2+\eta(\rho+\xi)))\gamma)t^5}{5!} \end{aligned} \tag{18}$$

$$
\begin{aligned}
I_2 &= \frac{(b^2p_1{p_2}^2 + (-p_1(\xi+\rho-p_2)\gamma + \chi(\wedge+\eta)p_2 + p_2)b)t^4}{4!} \\
&+\frac{p_1(\rho+\chi+\xi)bt^4}{4!} + \frac{(b^2p_2(\wedge+\eta)^2 + \chi\gamma(\wedge+\eta)))t^4}{4!} - \frac{(\wedge+\eta)^2b^2\gamma t^7}{7!} \\
&+\frac{(bdp_1p_2 + (\rho+\chi+\xi)^2\gamma)t^3}{3!} - \frac{(b(2p_2(\wedge+\eta)b - p_1\gamma)p_1)t^5}{5!} \\
&+\frac{(\rho+\chi+\xi)^2p_2t^2}{2!} - \frac{(-b^2((2p_1-p_2)\gamma + p_2(\wedge+\eta))(\wedge+\eta))t^6}{6!} \\
R_2 &= \frac{(bp_2p_1\xi - \xi(\rho+\chi+\xi)\gamma - \chi\gamma\xi)t^3}{3!} + \frac{(\xi p_1\gamma b + \xi(\wedge+\eta)p_2b)t^4}{4!} \\
&+\frac{\xi(\wedge+\eta)\gamma bt^5}{5!} - \frac{(\xi(\rho+\chi+\xi)p_2 + \chi\xi p_2 - \chi^2p_3)t^2}{2!}
\end{aligned} \tag{19}
$$

Subsequently, the remaining terms are computed using a similar approach. By employing these calculated values, we can approximate the solutions to the above systems in the form of an infinite series as:

$$
\begin{aligned}
S(t) &= S_0 + S_1 + S_2 + ... \\
I(t) &= I_0 + I_1 + I_2 + ... \\
R(t) &= R_0 + R_1 + R_2 + ...
\end{aligned}
$$

By using the initial conditions and the provided parameter values in Table 1, we get:

$$
\begin{aligned}
S(t) &= 222.002105 - 0.776103051t - 0.009519500822t^2 \\
&-0.0001301552435t^3 - 0.00005532499957t^4 - 0.00007962971005t^5 \\
&+2.510080030\times10^{-11}t^6 + 2.774293121\times10^{-15}t^7 + ... \\
I(t) &= 0.537176 + 0.00913530136t + 0.0002148468723t^2 \\
&+0.00004271085092t^3 + 0.00005522191855t^4 + 0.00007962968773t^5 \\
&-2.510080030\times10^{-11}t^6 - 2.774293121\times10^{-15}t^7 + ... \\
R(t) &= 0.482 - 0.001376872t - 0.00001780500560t^2 \\
&+0.00001190825128t^3 + 1.344535416\times10^{-8}t^4 \\
&+2.911503501\times10^{-12}t^5 + ...
\end{aligned} \tag{20}
$$

3.2. Differential transform method (DTM):. In this sub-section, we demonstrate the application of the differential transform method to the nonlinear ordinary differential system (1). The fundamental definitions and properties of the DTM are provided below.

Definition 1: Given an arbitrary funstion $u(x)$, then $u(x)$ can be expanded in a Taylor series about the point $x = 0$ as

$$
u(x) = \sum_{n=0}^{\infty} \frac{x^k}{k!}[\frac{d^ku(t)}{dx^k}]_{t=0}
$$

Definition 2: The differential transform $U(k)$ of a function $u(t)$ is defined as follows:

$$U(k) = \frac{1}{k!}[\frac{d^k u(t)}{dx^k}]_{t=0}$$

Definition 3: The inverse differential transform $u(t)$ is given as:

$$u(t) = \sum_{n=0}^{\infty} U^k t^k$$

TABLE 2. Properties of the DTM

Original functions	Transformed functions
$u(x) = \frac{dg(x)}{dx}$	$U(k) = (k+1)G(k+1)$
$u(x) = 1$	$U(k) = \delta(k)$, where δ is the kronecker delta
$u(x) = g(x)h(x)$	$U(k) = \sum_{j=0}^{k} G(j)H(k-j)$

By using the definitions and properties of the differential transform method, the (1) can be written as:

$$\begin{aligned} S(k+1) &= \frac{1}{k+1}[(\wedge + \eta)\delta(k) - \chi S(k) - b\sum_{j=0}^{k} S(j)I(k-j)] \\ I(k+1) &= \frac{1}{k+1}[b\sum_{j=0}^{k} S(j)I(k-j) + \gamma\delta(k) - (\rho + \chi + \xi)I(k)] \\ R(k+1) &= \frac{1}{k+1}[\xi I(k) - \chi R(k)] \end{aligned} \tag{21}$$

subject to the initial conitions:

$$S(0) = p_1, \quad I(0) = p_2, \quad R(0) = p_3 \tag{22}$$

The first iteration of the DTM is derived by setting $k = 0$ in (19).

$$\begin{aligned} S(1) &= (\wedge + \eta)\delta(0) - \chi S(0) - bS(0)I(0) \\ I(1) &= bS(0)I(0) + \gamma\delta(0) - (\rho + \chi + \xi)I(0) \\ R(1) &= \xi I(0) - \chi R(0) \end{aligned} \tag{23}$$

(or)

$$\begin{aligned} S(1) &= \wedge + \eta - \chi p_1 - bp_1p_2 \\ I(1) &= bp_1p_2 + \gamma - (\rho + \chi + \xi)p_2 \\ R(1) &= \xi p_2 - \chi p_3 \end{aligned} \tag{24}$$

The second iteration of the DTM is derived by setting $k = 1$ in (19).

$$\begin{aligned} S(2) &= \frac{1}{2}[(\wedge + \eta)\delta(1) - \chi S(1) - b(S(1)I(0) + S(0)I(1))] \\ I(2) &= \frac{1}{2}[b(S(1)I(0) + S(0)I(1)) + \gamma\delta(1) - (\rho + \chi + \xi)I(1)] \\ R(2) &= \frac{1}{2}[\xi I(1) - \chi R(1)] \end{aligned} \tag{25}$$

(or)

$$\begin{aligned} S(2) = \frac{1}{2}[&-\chi(\wedge + \eta - \chi p_1 - bp_1p_2) - b(p_1(bp_1p_2 + \gamma - (\rho + \chi + \xi)p_2) \\ &+(\wedge + \eta - \delta p_1 - bp_1p_2)p_2)] \\ I(2) = \frac{1}{2}[&b(p_1(bp_1p_2 + \gamma - (\rho + \chi + \xi)p_2) + (\wedge + \eta - \chi p_1 - bp_1p_2)p_2) \\ &-(\rho + \chi + \xi)(bp_1p_2 + \gamma - (\rho + \chi + \xi)p_2)] \\ R(2) = \frac{1}{2}[&\xi(bp_1p_2 + \gamma - (\rho + \chi + \xi)p_2) - \chi(\xi p_2 - \chi p_3)] \end{aligned} \tag{26}$$

Subsequently, the remaining terms are computed using a similar approach. By employing these calculated values, we can approximate the solutions to the above systems in the form of an infinite series as:

$$\begin{aligned} S(t) &= \sum_{n=0}^{\infty} S(k)t^k = S(0) + S(1)t + S(2)t^2 + ... \\ I(t) &= \sum_{n=0}^{\infty} I(k)t^k = I(0) + I(1)t + I(2)t^2 + ... \\ R(t) &= \sum_{n=0}^{\infty} R(k)t^k = R(0) + R(1)t + R(2)t^2 + ... \end{aligned}$$

By using the initial conditions and the provided parameter values in Table 1, we get:

$$\begin{aligned} S(t) &= 222.002105 - 0.7999538916t + 0.002320023054t^2 + ... \\ I(t) &= 0.537176 + 0.00913530136t - 0.00001056517630t^2 + ... \\ R(t) &= 0.482 - 0.001376872t + 0.00001797125524t^2 + ... \end{aligned} \tag{27}$$

4. Numerical Simulation

The numerical solution for the first-order nonlinear differential system (1) was obtained using a hybrid approach, the ode45 solver and MATLAB software (Appendix). To assess the accuracy of the obtained solution, a comparison was made between the numerical results and the analytical solutions obtained through the Laplace Adomian decomposition and differential transform methods. Graphical illustrations of the analytical concentrations S, I, and R are presented in Figures 2, 3, 4, 5 alongs with their corresponding numerical outcomes, encompassing

a comprehensive range of parameter values. A comparison between these two datasets demonstrated a significant level of concordance between the approximated analytical solutions and numerical results. The accuracy of our analytical expressions for the concentrations S, I, and R, based on the different parameter values, is presented in Tables 3, 4, 5, 6, 7, 8, 9, 10, 11. Both the analytical results emphasize a good agreement with the outcomes obtained from the numerical simulations and the overall error between LADM and DTM with the numerical simulation does not exceed 0.06% and 0.007% respectively.

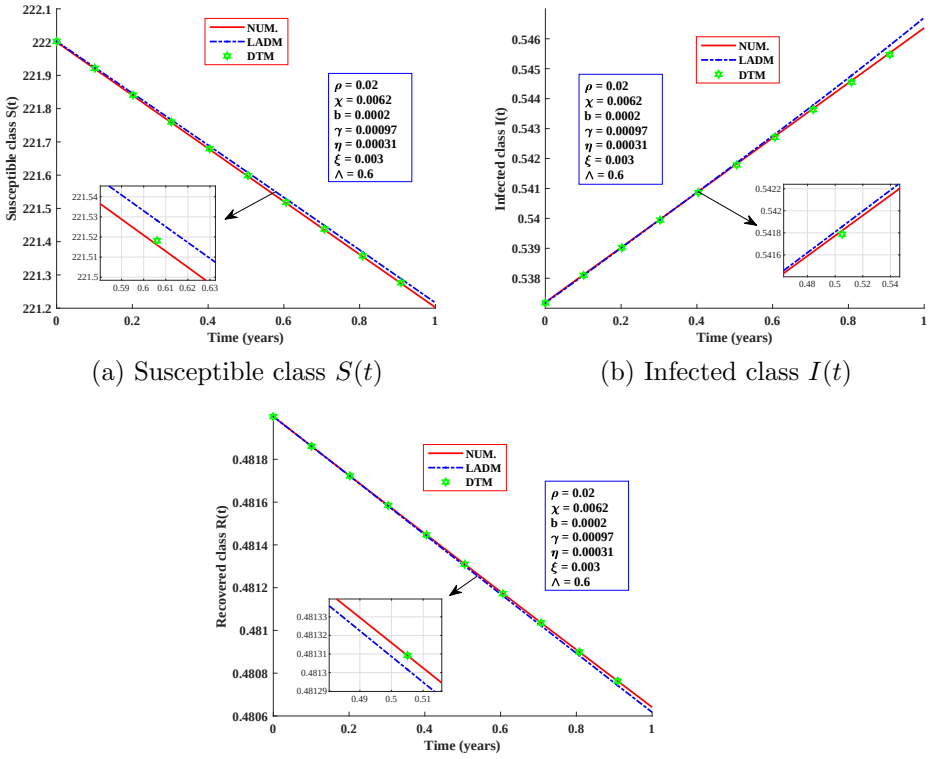

(a) Susceptible class $S(t)$

(b) Infected class $I(t)$

(c) Recovered class $R(t)$

FIGURE 2. Comparison of semi-analytical expressions obtained by LADM and DTM with numerical simulation for the parameters provided in Table 1.

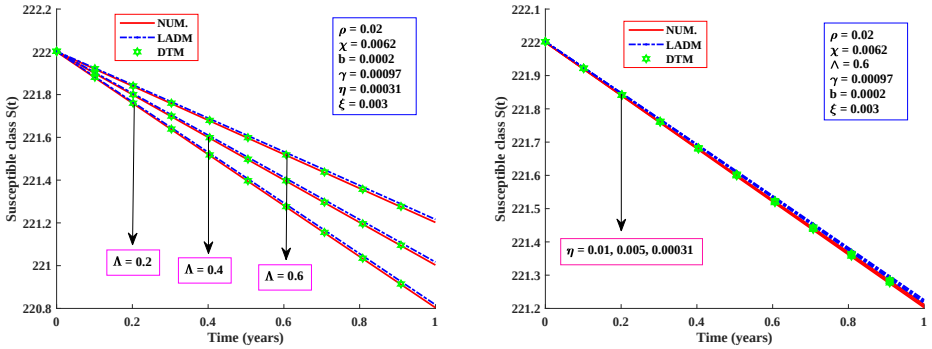

(a) (b)

FIGURE 3. Comparison of analytical and numerical solutions for the concentration $S(t)$, when (a) $\wedge = 0.2$ to 0.6 and other parameters $\chi, b, \gamma, \eta, \xi, \rho$ are fixed, (b) $\eta = 0.00031$ to 0.01 and other parameters $\chi, b, \gamma, \wedge, \xi, \rho$ are fixed.

TABLE 3. Comparison between the Laplace Adomian Decomposition Method (LADM) and Differential Transform Method (DTM) with the numerical outcomes for the concentration profile, Susceptible $S(t)$

Susceptible class $S(t)$					
t	Num.	LADM	DTM	LADM Error%	DTM Error%
0	222.0021	222.0021	222.0021	0.0000	0.0000
0.1	221.9221	221.9243	221.9221	0.0009	0.0000
0.2	221.8421	221.8465	221.8422	0.0019	0.0000
0.3	221.7620	221.7684	221.7623	0.0028	0.0001
0.4	221.6817	221.6901	221.6824	0.0037	0.0003
0.5	221.6012	221.6116	221.6027	0.0046	0.0006
0.6	221.5204	221.5329	221.5229	0.0056	0.0011
0.7	221.4393	221.4540	221.4432	0.0066	0.0017
0.8	221.3577	221.3750	221.3636	0.0078	0.0026
0.9	221.2756	221.2952	221.2840	0.0088	0.0037
1	221.1929	221.2162	221.2044	0.0105	0.0051
Average Error %				0.0048	0.0013

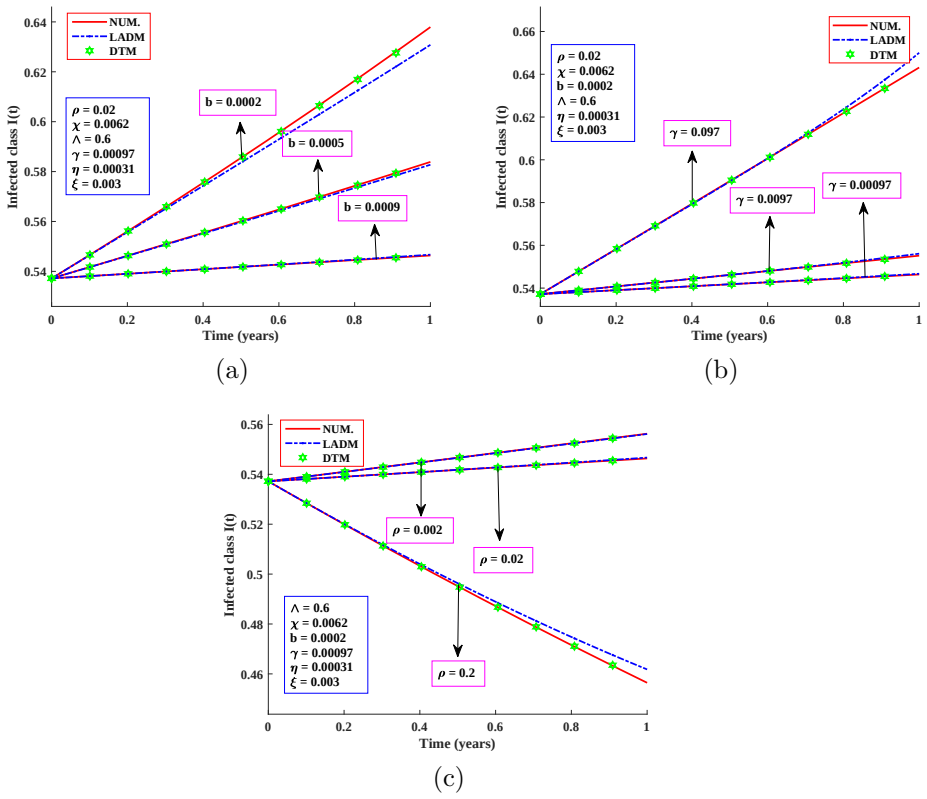

FIGURE 4. Comparison of analytical and numerical solutions for the concentration $I(t)$, when (a) $b = 0.0002$ to 0.0009 and other parameters $\chi, \wedge, \gamma, \eta, \xi, \rho$ are fixed, (b) $\gamma = 0.00097$ to 0.097 and other parameters $\chi, b, \eta, \wedge, \xi, \rho$ are fixed, (c) $\rho = 0.002$ to 0.2 and other parameters $\chi, b, \gamma, \wedge, \xi, \eta$ are fixed.

5. Discussion

The Laplace Adomian decomposition method (LADM) and differential transform method (DTM) was used to solve the nonlinear equations governing the concentrations of susceptible, infected, and recovered individuals in SARS-CoV-2 model. Comparative analyses were conducted among LADM, DTM, and numerical simulations under varying parameter values in the model. The results are effectively presented through graphical figures and informative tables, demonstrating the efficacy and accuracy of both the LADM and DTM. Upon analyzing the figures and tables, it becomes evident that within the designated time interval, the DTM consistently provides a superior approximation compared to the

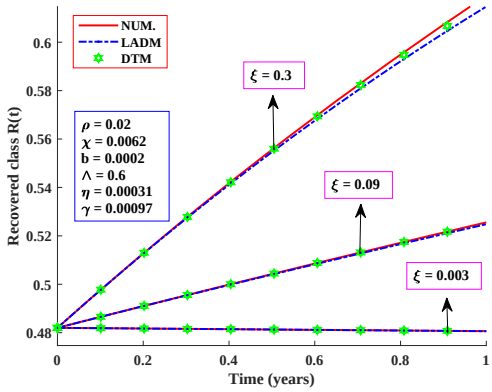

FIGURE 5. Comparison of analytical and numerical solutions for the concentration $R(t)$, when $\xi = 0.003$ to 0.3 and other parameters $\chi, b, \gamma, \eta, \wedge, \rho$ are fixed.

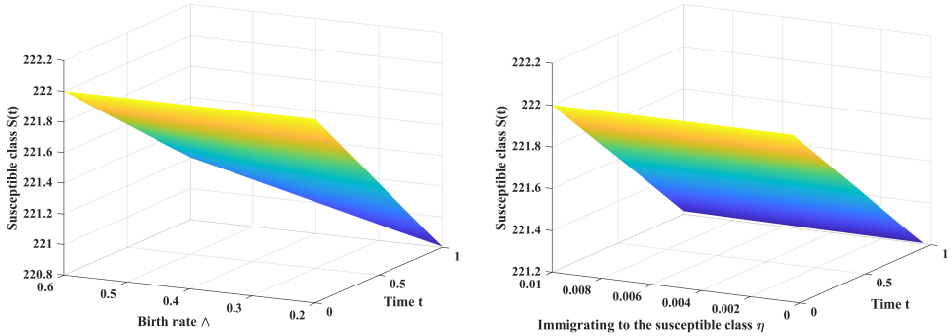

(a) (b)

FIGURE 6. Susceptible SARS-CoV-2 model using different values of the parameters $\wedge$ and η.

LADM with the simulations. Importantly, as the numerical values of the SARS-CoV-2 model increased, both methods converge toward the numerical simulation of the model. However, DTM effectively captures this behavior, even with a limited time interval.

Figure 2.a depicts the susceptible class $S(t)$, utilizing the provided parameters in Table 1. The susceptible population that are in contact with the disease are exposed to the infected population. The impact of these parameters becomes evident as the susceptible class exhibited a decreasing trend. Table 3 provides a comparison between the numerical and analytical results for the susceptible

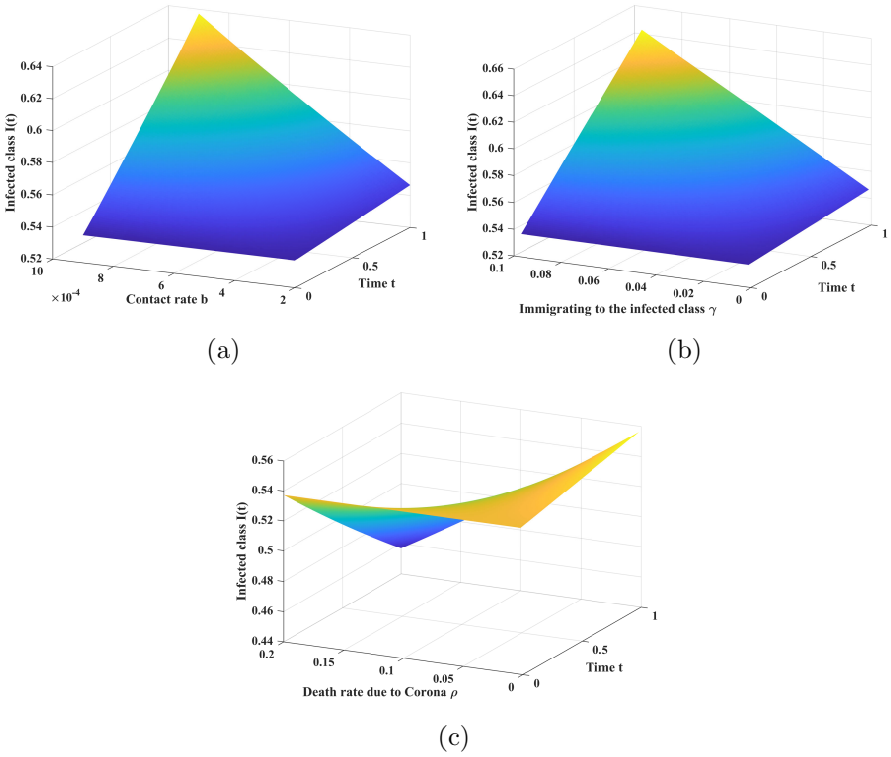

FIGURE 7. Infected SARS-CoV-2 model using different values of the parameters b, γ and ρ.

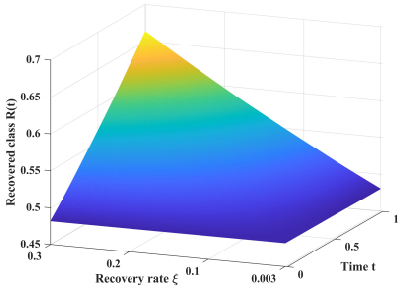

FIGURE 8. Recovered SARS-CoV-2 model using different values of the parameter ξ.

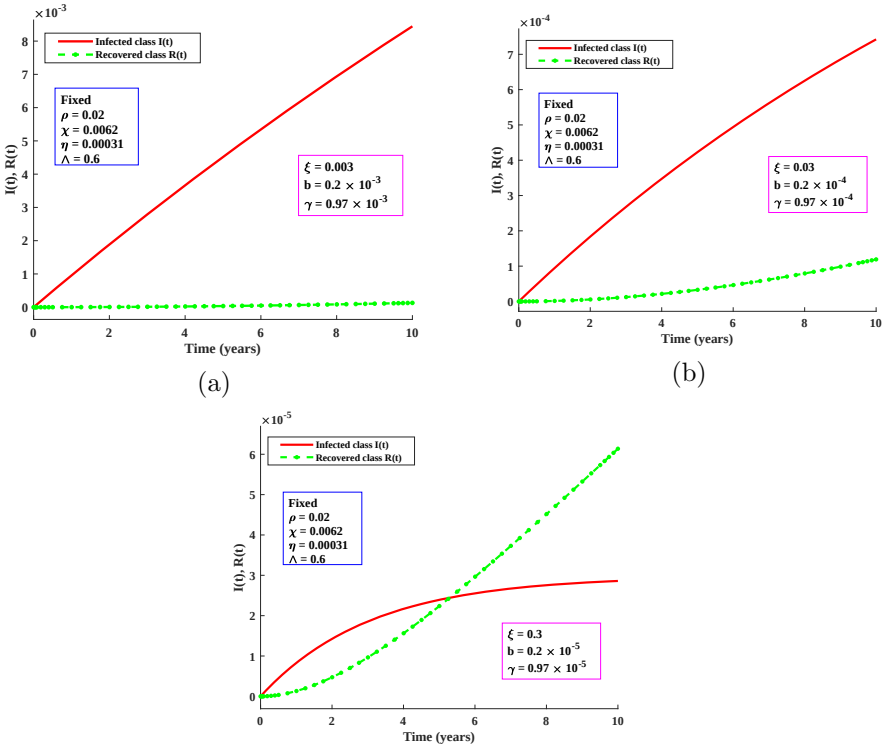

FIGURE 9. Impact of the parameters ξ, b and γ on the Infected and Recovered classes, when (a) $\xi = 0.003$, $b = 0.2 \times 10^{-3}$ and $\gamma = 0.97 \times 10^{-3}$, (b) $\xi = 0.03$, $b = 0.2 \times 10^{-4}$ and $\gamma = 0.97 \times 10^{-4}$, (c) $\xi = 0.3$, $b = 0.2 \times 10^{-5}$ and $\gamma = 0.97 \times 10^{-5}$.

class $S(t)$. Figure 2.b depicts the infected class $I(t)$. The impact of these parameters becomes evident as the infected class exhibited an increasing trend, as the number of individuals immigrating from susceptible to infection class. Table 4 provides a comparison between the numerical and analytical results for the infected class $I(t)$. Figure 2.c depicts the recovered class $R(t)$. The impact of these parameters is evident as the recovered class shows a decreasing trend, this is because infected class may not have better progression rates. Table 5 provides a comparison between the numerical and analytical results for the recovered class $R(t)$.

In Figure 3.a, when fixing the parameters $\chi, b, \gamma, \eta, \xi, \rho$ and increasing $\wedge$, the

TABLE 4. Comparison between the Laplace Adomian Decomposition Method (LADM) and Differential Transform Method (DTM) with the numerical outcomes for the concentration profile, Infected $I(t)$

Infected class $I(t)$					
t	Num.	LADM	DTM	LADM Error%	DTM Error%
0	0.5372	0.5371	0.5371	0.0186	0.0186
0.1	0.5381	0.5380	0.5380	0.0185	0.0185
0.2	0.5390	0.5390	0.5390	0.0000	0.0000
0.3	0.5399	0.5399	0.5399	0.0000	0.0000
0.4	0.5408	0.5408	0.5408	0.0000	0.0000
0.5	0.5417	0.5418	0.5417	0.0184	0.0000
0.6	0.5426	0.5427	0.5426	0.0184	0.0000
0.7	0.5435	0.5437	0.5435	0.0210	0.0000
0.8	0.5445	0.5446	0.5444	0.0215	0.0183
0.9	0.5454	0.5456	0.5453	0.0216	0.0183
1	0.5463	0.5467	0.5463	0.0327	0.0000
Average Error %				0.0135	0.0067

TABLE 5. Comparison between the Laplace Adomian Decomposition Method (LADM) and Differential Transform Method (DTM) with the numerical outcomes for the concentration profile, Recovered $R(t)$

Recovered class $R(t)$					
t	Num.	LADM	DTM	LADM Error%	DTM Error%
0	0.4820	0.4820	0.4820	0.0000	0.0000
0.1	0.4819	0.4818	0.4818	0.0207	0.0207
0.2	0.4817	0.4817	0.4817	0.0000	0.0000
0.3	0.4815	0.4815	0.4815	0.0000	0.0000
0.4	0.4814	0.4814	0.4814	0.0000	0.0000
0.5	0.4813	0.4813	0.4813	0.0000	0.0000
0.6	0.4811	0.4811	0.4811	0.0000	0.0000
0.7	0.4810	0.4810	0.4810	0.0000	0.0000
0.8	0.4809	0.4808	0.4809	0.0207	0.0000
0.9	0.4807	0.4807	0.4807	0.0000	0.0000
1	0.4806	0.4806	0.4806	0.0000	0.0000
Average Error %				0.0037	0.0018

susceptible class also increases. In Figure 3.b, when η increases and other parameters are fixed, there is no variation in the susceptible class. In Figure 4.a, when fixing the parameters $\chi, \wedge, \gamma, \eta, \xi, \rho$ and increasing b, the infected class also increases. In Figure 4.b, when γ increases and other parameters are fixed, the infected class increases. In Figure 4.c, when ρ increases and other parameters are fixed, the infected class decreases. In Figure 5, when fixing the parameters $\chi, b, \gamma, \eta, \wedge, \rho$ and increasing ξ, the recovered class also increases.

TABLE 6. Results of birth rate $\wedge$ versus Susceptible class $S(t)$ at $t = 0.5$

S. No	$\wedge$	Num.	LADM	DTM	LADM Error%	DTM Error%
1	0.2	221.403	221.412	221.403	0.0040	0.0000
2	0.4	221.503	221.512	221.503	0.0040	0.0000
3	0.6	221.600	221.612	221.603	0.0054	0.0013
Average Error %					0.0044	0.0003

TABLE 7. Results of rate of individuals immigrating to the susceptible class η versus Susceptible class $S(t)$ at $t = 0.5$

S. No	η	Num.	LADM	DTM	LADM Error%	DTM Error%
1	0.01	221.608	221.616	221.608	0.0036	0.0000
2	0.005	221.605	221.614	221.605	0.0040	0.0000
3	0.0003	221.600	221.612	221.603	0.0054	0.0013
Average Error %					0.0043	0.0003

TABLE 8. Results of rate of individuals immigrating to the infected class γ versus Infected class $I(t)$ at $t = 0.5$

S. No	γ	Num.	LADM	DTM	LADM Error%	DTM Error%
1	0.097	0.590	0.590	0.590	0.0000	0.0000
2	0.0097	0.546	0.546	0.546	0.0000	0.0000
3	0.00097	0.542	0.542	0.542	0.0000	0.0000
Average Error %					0.0000	0.0000

TABLE 9. Results of contact rate b versus Infected class $I(t)$ at $t = 0.5$

S. No	b	Num.	LADM	DTM	LADM Error%	DTM Error%
1	0.0002	0.542	0.542	0.542	0.0000	0.0000
2	0.0005	0.560	0.560	0.560	0.0000	0.0000
3	0.0009	0.585	0.584	0.585	0.1709	0.0000
Average Error %					0.0427	0.0000

TABLE 10. Results of death rate due to corona ρ versus Infected class $I(t)$ at $t = 0.5$

S. No	ρ	Num.	LADM	DTM	LADM Error%	DTM Error%
1	0.002	0.547	0.547	0.547	0.0000	0.0000
2	0.02	0.560	0.560	0.560	0.0000	0.0000
3	0.2	0.495	0.496	0.495	0.2020	0.0000
Average Error %					0.0505	0.0000

TABLE 11. Results of recovery rate ξ versus Recovered class $R(t)$ at $t = 0.5$

S. No	ξ	Num.	LADM	DTM	LADM Error%	DTM Error%
1	0.003	0.481	0.481	0.481	0.0000	0.0000
2	0.09	0.504	0.504	0.504	0.0000	0.0000
3	0.3	0.556	0.555	0.556	0.1798	0.0000
Average Error %					0.0599	0.0000

In Figures 6.a - 6.b, the parameters $\wedge$ and η against time t increases as the susceptible class also increases. Tables 6 and 7 provides the results of $\wedge$ and η versus susceptible class at time $t = 0.5$ respectively. In Figures 7.a - 7.b, the parameters b and γ against time t increases as the infected class also increases, but in Figure 7.c, the parameter ρ against time t increases as the infected class decreases. Tables 8, 9 and 10 provides the results of b, γ and ρ versus infected class at time $t = 0.5$ respectively. In Figure 8, the parameter ξ against time t increases as the recovered class also increases. Table 11 provides the results of ξ versus recovered class at time $t = 0.5$.
The recovery rate ξ, contact rate b, and the rate of individuals immigrating to the infected class γ, plays a crucial role in overcoming infection. In Figure 9.a, we illustrate the initial state solution for the infected and recovered individuals. Subsequently, Figures 9.b - 9.c depicts the impact of varying parameters of ξ, b and γ. When increasing the parameter ξ and reducing the parameters b and γ simultaneously, we observe an improved recovery population.

6. Conclusion

In this study, we derived an semi-analytical solutions for the SIR framework of SARS-CoV-2 model using both the Laplace Adomian decomposition method and the differential transform approach. A comprehensive comparison between the analytical and numerical results was conducted, which yields more favorable results. The findings revealed distinct behaviors among the three derivative classes when applying the LADM, DTM, and the numerical approach. The Tables 3-11 and Figures 2-5 demonstrate the effectiveness of LADM and DTM in solving nonlinear equations. DTM manages to capture this behaviour quite well, considering the short time interval. Our focus was on analyzing the parameters ξ, b and γ to reduce the infected class $I(t)$ and to increase the recovered class $R(t)$. Initially, the infected class reaches peak as the impact of the parameters, yet the recovered class experiences growth in the SARS-CoV-2 model over time t.

7. Appendix

MATLAB program for numerical simulation (1) with initial conditions (2)

```
function SARS
options=odeset ('RelTol',1e-6,'Stats','on');
%initial conditions
Xo=[222.002105; 0.537176; 0.482];
tspan=[0,1];
tic
[t, X] = ode45(@TestFunction, tspan, Xo, options);
%-----------------------------------------------------
figure
hold on
plot(t, X(:,1),'-')
plot(t, X(:,2),'-')
plot(t, X(:,3),'-')
legend('x1','x2','x3')
ylabel('x')
xlabel('t')
return
%-----------------------------------------------------
function [dx_dt]= TestFunction(t,x)
wedge=0.6; eta=0.00031; b=0.0002; gamma=0.00097; xi=0.003; chi=0.0062;
rho=0.02;
dx_dt(1)=wedge+eta-chi*x(1)-b*x(1)*x(2);
dx_dt(2)=b*x(1)*x(2)+gamma-(rho+chi+xi)*x(2);
dx_dt(3)=xi*x(2)-chi*x(3);
dx_dt=dx_dt';
return
```

Conflicts of interest : The authors declare no conflict of interest.

Data availability : Not applicable

Acknowledgments : The authors wish to thank Tshwane University of Technology for their financial support and the Madura college for their continuous support and encouragement.

References

1. WHO, Coronavirus disease (COVID-19). https://www.who.int/emergencies/diseases/novel-coronavirus-2019.

2. B. Hu, P. Ning, J. Qiu, V. Tao, A.T. Devlin, H. Chen, J. Wang, & H. Lin, *Modeling the complete spatiotemporal spread of the COVID-19 epidemic in mainland China*, International Journal of Infectious Diseases **110** (2021), 247–257.
3. M. Hasoksuz, S. Kilic, & F. Sarac, *Coronaviruses and SARS-COV-2*, Turkish Journal of Medical sciences **50** (2020), 549–556.
4. M.A. Johansson, T.M. Quandelacy, S. Kada, P.V. Prasad, M. Steele, J.T. Brooks, R.B. Slayton, M. Biggerstaff, & J.C. Butler, *SARS-CoV-2 Transmission From People Without COVID-19 Symptoms*, JAMA Network Open **4** (2021), e2035057.
5. S. Zhao, Q. Lin, J. Ran, S.S. Musa, G. Yang, W. Wang, Y. Lou, D. Gao, L. Yang, D. He, & M.H. Wang, *Preliminary estimation of the basic reproduction number of novel coronavirus (2019-nCoV) in China, from 2019 to 2020: A data-driven analysis in the early phase of the outbreak*, International Journal of Infectious Diseases **92** (2020), 214–217.
6. N.G. Davies, S. Abbott, R.C. Barnard, C.I. Jarvis, A.J. Kucharski, J.D. Munday, C.A.B. Pearson, T.W. Russell, D.C. Tully, A.D. Washburne, T. Wenseleers, A. Gimma, W. Waites, K.L.M. Wong, K. Van Zandvoort, J.D. Silverman, K. Diaz-Ordaz, R. Keogh, R.M. Eggo, W.J. Edmunds, *Estimated transmissibility and impact of SARS-CoV-2 lineage B.1.1.7 in England*, Science **372** (2021), 6538.
7. Y. Liu, A.A. Gayle, A. Wilder-Smith, & J. Rocklöv, *The reproductive number of COVID-19 is higher compared to SARS coronavirus*, Journal of Travel Medicine **27** (2020), 2.
8. M. Veera Krishna, *Mathematical modelling on diffusion and control of COVID–19*, Infectious Disease Modelling **5** (2020), 588–597.
9. D. Martínez-Rodríguez, G. Gonzalez-Parra, & R. Villanueva, *Analysis of Key Factors of a SARS-CoV-2 Vaccination Program: A Mathematical Modeling Approach*, Epidemiologia **2** (2021), 140–161.
10. G. Gonzalez-Parra, D. Martínez-Rodríguez, & R. Villanueva-Micó, *Impact of a New SARS-CoV-2 Variant on the Population: A Mathematical Modeling Approach*, Mathematical and Computational Applications **26** (2021), 25.
11. M. Makhoul, H.H. Ayoub, H. Chemaitelly, S. Seedat, G.R. Mumtaz, S. Al-Omari, & L.J. Abu-Raddad, *Epidemiological Impact of SARS-CoV-2 Vaccination: Mathematical Modeling Analyses*, Vaccines **8** (2020), 668.
12. A. Salimipour, T. Mehraban, H.S. Ghafour, N.I. Arshad, & M. Ebadi, *RETRACTED: SIR model for the spread of COVID-19: A case study*, Operations Research Perspectives **10** (2023), 100265.
13. I. Cooper, A. Mondal, & C.G. Antonopoulos, *A SIR model assumption for the spread of COVID-19 in different communities*, Chaos, Solitons & Fractals **139** (2020), 110057.
14. M. D'Arienzo, & A. Coniglio, *Assessment of the SARS-CoV-2 basic reproduction number, R0, based on the early phase of COVID-19 outbreak in Italy*, Biosafety and Health **2** (2020), 57–59.
15. M. Ahumada, A. Ledesma-Araujo, L. Gordillo, & J. Marín, *Mutation and SARS-CoV-2 strain competition under vaccination in a modified SIR model*, Chaos, Solitons & Fractals **166** (2023), 112964.
16. A. McMahon, & N.C. Robb, *Reinfection with SARS-CoV-2: Discrete SIR (Susceptible, Infected, Recovered) Modeling Using Empirical Infection Data*, JMIR Public Health and Surveillance **6** (2020), e21168
17. M. Venkatasen, S.K. Mathivanan, P. Jayagopal, P. Mani, S. Rajendran, U. Subramaniam, A.C. Ramalingam, V.A. Rajasekaran, A. Indirajithu, & M. Sorakaya Somanathan, *Forecasting of the SARS-CoV-2 epidemic in India using SIR model, flatten curve and herd immunity*, Journal of Ambient Intelligence and Humanized Computing (2020), 1-9.
18. C. Roberto Telles, H. Lopes, & D. Franco, *SARS-COV-2: SIR Model Limitations and Predictive Constraints*, Symmetry **13** (2021), 676.
19. Z.W. Tong, Y.P. Lv, R.U. Din, I. Mahariq, & G. Rahmat, *Global transmission dynamic of SIR model in the time of SARS-CoV-2*, Results in Physics **25** (2021), 104253.

20. I. Sahu, & S.R. Jena, *SDIQR mathematical modelling for COVID-19 of Odisha associated with influx of migrants based on Laplace Adomian decomposition technique*, Modeling Earth Systems and Environment **9** (2023), 4031–4040.
21. A. Raza, M. Farman, A. Akgül, M.S. Iqbal, A. Ahmad, *Simulation and numerical solution of fractional order Ebola virus model with novel technique[J]*, AIMS Bioengineering **7** (2020), 194-207.
22. P. Pue-on, *Laplace Adomian decomposition method for solving Newell-Whitehead-Segel equation*, Applied Mathematical Sciences **7** (2013), 6593–6600.
23. Liberty Ebiwareme, Fun-Akpo Pere Kormane, & Edmond Obiem Odok, *Simulation of unsteady MHD flow of incompressible fluid between two parallel plates using Laplace-Adomian decomposition method*, World Journal of Advanced Research and Reviews **14** (2022), 136–145.
24. F. Haq, K. Shah, G.U. Rahman, Y. Li, & M. Shahzad, *Computational Analysis of Complex Population Dynamical Model with Arbitrary Order*, Complexity (2018), 1–8.
25. J. Xu, H. Khan, R. Shah, A. Alderremy, S. Aly, & D. Baleanu, *The analytical analysis of nonlinear fractional-order dynamical models*, AIMS Mathematics **6** (2021), 6201–6219.
26. N. Jeeva, K.M. Dharmalingam, *Mathematical analysis of new SEIQR model via Laplace Adomian decomposition method*, Indian Journal of Natural Science **15**, (2024) 72148-72157.
27. M. Thongmoon, & S. Pusjuso, *The numerical solutions of differential transform method and the Laplace transform method for a system of differential equations*, Nonlinear Analysis: Hybrid Systems **4** (2010), 425–431.
28. A. Harir, S. Melliani, H. El Harfi, & L.S. Chadli, *Variational Iteration Method and Differential Transformation Method for Solving the SEIR Epidemic Model*, International Journal of Differential Equations (2020), 1–7.
29. A.M. Batiha, B. Batiha, *A new method for solving epidemic model*, Aust. J. Basic Appl. Sci. **5** (2011), 3122–3126.
30. B. Batiha, *The solution of the prey and predator problem by differential transformation method*, Int. J. Basic Appl. Sci. **4** (2015), 36.
31. A. Adeniji, O. Mogbojuri, M. Kekana, & S. Fadugba, *Numerical solution of rotavirus model using Runge-Kutta-Fehlberg method, differential transform method and Laplace Adomian decomposition method*, Alexandria Engineering Journal **82** (2023), 323–329.

N. Jeeva received M.Sc from the American College and currently pursuing Ph.D. at the Madura College. His research interests are numerical analysis and semi-analytical solutions for epidemiological models.

PG and Research Department of Mathematics, The Madura College (affiliated to Madurai Kamaraj University), Madurai, Tamil Nadu, India.
e-mail: jeevapirc2405@gmail.com

K.M. Dharmalingam received Ph.D from Madurai Kamaraj University. He is currently a Associate professor at the Madura College. His research interest is in Differential equations, Graph theory and Topology.

PG and Research Department of Mathematics, The Madura College (affiliated to Madurai Kamaraj University), Madurai, Tamil Nadu, India.
e-mail: kmdharma6902@yahoo.in

S.E. Fadugba received his Ph.D. from University of Ibadan, Nigeria. He is currently a Senior Lecturer in the Department of Mathematics, Ekiti State University, Ado Ekiti, Nigeria, His research interest spans across Numerical Analysis, Financial Mathematics, Fractional Calculus and Mathematical Modelling. He is skilled in Lecturing, Curriculum Development, Quality Assurance and Academic Writing.

Department of Mathematics, Ekiti State University, Ado Ekiti, 360001, Nigeria.
e-mail: sunday.fadugba@eksu.edu.ng

M.C. Kekana received his Ph.D. from Tshwane University of Technology. He is currently a senior lecturer and section head, and a researcher at the university. His research interest is in numerical analysis, Skilled in Lecturing, Curriculum Development, Academic Writing, Distance Learning, and Science.

Department of Mathematics and Statistics, Tshwane University of Technology, Pretoria, South Africa.
e-mail: kekanaMC@tut.ac.za

A.A. Adeniji received his Ph.D. from Tshwane University of Technology. His areas of interest in study include infectious diseases, epidemiological models, and numerical analysis of dynamical systems. In order to inform policies, he also investigates mathematical models for sociological issues. He engages lecturing with strong eclectic ability.

Department of Mathematics and Statistics, Tshwane University of Technology, Pretoria, South Africa.
e-mail: adejimi.adeniji@gmail.com, Adenijiaa@tut.ac.za